10-2016

Pyrimidine Pathway-Dependent and -Independent Functions of the Toxoplasma gondii Mitochondrial Dihydroorotate Dehydrogenase

Miryam Andrea Hortua Triana
Dartmouth College

Daniela Cajiao Herrera
University of Los Andes, Colombia

Barbara H. Zimmermann
University of Los Andes, Colombia

Barbara A. Fox
Dartmouth College

David Bzik
Dartmouth College

AMERICAN SOCIETY FOR MICROBIOLOGY | Infection and Immunity

Pyrimidine Pathway-Dependent and -Independent Functions of the *Toxoplasma gondii* Mitochondrial Dihydroorotate Dehydrogenase

Miryam Andrea Hortua Triana,[a]* Daniela Cajiao Herrera,[b] Barbara H. Zimmermann,[b] Barbara A. Fox,[a] David J. Bzik[a]

Department of Microbiology and Immunology, Geisel School of Medicine at Dartmouth, Lebanon, New Hampshire, USA[a]; Departamento de Ciencias Biológicas, Universidad de los Andes, Bogotá, Colombia[b]

Dihydroorotate dehydrogenase (DHODH) mediates the fourth step of *de novo* pyrimidine biosynthesis and is a proven drug target for inducing immunosuppression in therapy of human disease as well as a rapidly emerging drug target for treatment of malaria. In *Toxoplasma gondii*, disruption of the first, fifth, or sixth step of *de novo* pyrimidine biosynthesis induced uracil auxotrophy. However, previous attempts to generate uracil auxotrophy by genetically deleting the mitochondrion-associated DHODH of *T. gondii* (*Tg*DHODH) failed. To further address the essentiality of *Tg*DHODH, mutant gene alleles deficient in *Tg*DHODH activity were designed to ablate the enzyme activity. Replacement of the endogenous *DHODH* gene with catalytically deficient *DHODH* gene alleles induced uracil auxotrophy. Catalytically deficient *Tg*DHODH localized to the mitochondria, and parasites retained mitochondrial membrane potential. These results show that *Tg*DHODH is essential for the synthesis of pyrimidines and suggest that *Tg*DHODH is required for a second essential function independent of its role in pyrimidine biosynthesis.

Toxoplasma gondii is an obligate intracellular parasite with an extremely broad host range (1). Primary infection during pregnancy can cause fetal death or severe congenital disease (2). Reactivated infection causes recurrent ocular toxoplasmosis (3), and during AIDS or immune suppression, reactivation of chronic infection causes severe and difficult-to-treat toxoplasmic encephalitis (4). Current drug treatment regimens for toxoplasmosis are poorly tolerated and have limited efficacy on chronic cyst stages (4, 5); thus, alternative therapeutic options are urgently needed.

Many of the clinically relevant drugs used to treat *Toxoplasma* infections, as well as related *Plasmodium* parasites that cause malaria, directly or indirectly target pyrimidine metabolism (6). The *de novo* pyrimidine biosynthetic pathway possesses several potential new drug targets (7). The fourth step of the pyrimidine biosynthetic pathway, mediated by dihydroorotate dehydrogenase (DHODH), is of interest because current therapeutic treatments target the human DHODH and *Plasmodium* parasites lack the ability to salvage pyrimidines; thus, the *de novo* pyrimidine pathway is the only source of pyrimidines for *Plasmodium* cell growth (6, 8, 9). Recently, the triazolopyrimidine DMS265 was advanced to clinical development as an antimalarial drug based on important characteristics such as extended bloodstream half-life, high selectivity toward the parasite enzyme, and excellent tolerability (10). Recently described triazolopyrimidine analogs exhibit even greater selectivity and efficiency against *Plasmodium* DHODH than does DSM265 (11).

In contrast to *Plasmodium* species, *T. gondii* has the ability not only to synthesize pyrimidines *de novo* (12) but also to salvage pyrimidines by first converting pyrimidine nucleosides to uracil, which is incorporated into the crucial pyrimidine pool as UMP by a uracil phophoribosyltransferase activity (13, 14), though this salvage pathway is not essential for acute (14, 15) or chronic (16) infection. Genetic deletion of the first, fifth, or sixth step of the pyrimidine biosynthetic pathway in *T. gondii* induced severe uracil auxotrophy, virulence attenuation, and undetectable chronic infection (16–19). The *T. gondii* DHODH (*Tg*DHODH), like the *Plasmodium* and human DHODH enzymes, resembles the family 2 DHODH enzymes (20, 21). Family 2 DHODH is monomeric and membrane associated and localizes to the inner mitochondrial membrane in both *Toxoplasma* and *Plasmodium* (22, 23). Family 2 DHODHs are coupled to the respiratory chain through ubiquinone-mediated reoxidation of DHODH, and electrons from oxidation of dihydroorotate enter the respiratory chain (24).

Chemical inhibitors of *Tg*DHODH activity *in vitro* were previously identified, and inhibitor profiles and bioinformatic analysis suggested that the enzyme was a potentially selective target for chemical inhibition (22). However, previous attempts to genetically delete the *TgDHODH* gene to create a uracil-auxotrophic mutant and to demonstrate the essentiality of this gene and activity were unsuccessful (22). Here, we examined the essential functions of *Tg*DHODH through the development of catalytically deficient *TgDHODH* gene alleles. We found that deletion of the endogenous *TgDHODH* gene to generate uracil auxotrophy was feasible only if the endogenous gene was replaced with a catalytically deficient *TgDHODH* gene allele. These results suggest that *Tg*DHODH is essential for two reasons, generation of the essential pyrimidine pools and another essential role in mitochondrial

Received 1 March 2016 **Returned for modification** 30 March 2016
Accepted 25 July 2016

Accepted manuscript posted online 1 August 2016

Citation Hortua Triana MA, Cajiao Herrera D, Zimmermann BH, Fox BA, Bzik DJ. 2016. Pyrimidine pathway-dependent and -independent functions of the *Toxoplasma gondii* mitochondrial dihydroorotate dehydrogenase. Infect Immun 84:2974–2981. doi:10.1128/IAI.00187-16.

Editor: J. H. Adams, University of South Florida

Address correspondence to David J. Bzik, david.j.bzik@dartmouth.edu.

* Present address: Miryam Andrea Hortua Triana, Center for Tropical and Emerging Global Disease, University of Georgia, Athens, Georgia, USA.

Supplemental material for this article may be found at http://dx.doi.org/10.1128/IAI.00187-16.

function or physiology that is not directly dependent on the DHODH enzyme activity.

MATERIALS AND METHODS

Culture conditions and strains. All parasite strains were continuously maintained *in vitro* by serial passage in Eagle modified essential medium supplemented with 1% fetal bovine serum in diploid human foreskin fibroblasts (HFF) at 36°C (25). Pyrimidine auxotrophs were supplemented with uracil (250 μM) (26). Targeted genetic manipulation of *T. gondii* was performed using the nonhomologous-recombination-deficient type I RH Δ*ku80* knockout strain (27).

Transformation, selection, and gene replacement validation. Prior to transfection, all plasmids were linearized at the 5′ end using the unique PmeI restriction enzyme site incorporated into the targeting plasmids. Approximately 15 μg of plasmid DNA was transfected into *T. gondii* strain RH Δ*ku80* Δ*hxgprt* (27) using a model BTX600 electroporator. Selection for integration of the targeting plasmid was performed in mycophenolic acid (MPA) (25 μg/ml) and xanthine (50 μg/ml). *Tg*DHODH mutant strains were also selected in the presence of uracil supplementation (250 μM) (18). Stable MPA-resistant clones were isolated, and genomic DNA was prepared with a DNA blood minikit (Qiagen) using a Qiacube automated robotic workstation. PCR products were amplified using a 1:1 mixture of *Taq* DNA polymerase and Expand long-template polymerase (Roche).

The PCR validation strategy was designed to measure the following: (i) PCR1, loss of intron 2 and absence of the endogenous *TgDHODH* gene, (ii) PCR2A and PCR2B*, correct integration of the targeting DNA, (iii) PCR3, loss of intron 11 and absence of the endogenous *DHODH* gene, (iv) PCR 4, correct 5′ target integration, and (v) PCR5, correct 3′ target integration. DNA primers used to construct plasmids for genetic manipulations and validation of progeny genotypes are shown in Table S1 in the supplemental material.

Site-directed mutagenesis. The previously reported cDNA (the pET19b-*Tg*DHODH-VSSM plasmid [22], here designated pET19b-WT) encoding active wild-type *Tg*DHODH enzyme was used as the template to build three mutant versions of DHODH. Mutagenesis was performed with the Stratagene QuikChange XS site-directed mutagenesis kit in order to mutate both N365 (pET19b-N365A) and N468 (pET19b-N468A) into an alanine. The N365/N468 double mutant (pET19b-N365A/N468A) was constructed using the pET19b-N468A expression plasmid. Oligonucleotide primers used to make the DHODH enzymes with single point mutations are listed in Table S1 in the supplemental material. Mutations were confirmed by DNA sequencing.

Gene-targeting plasmid constructs. Plasmid constructs used for gene replacement at the *TgDHODH* gene locus were developed in the yeast shuttle vector pRS416. Three distinct genetic elements were amplified by PCR and fused in the correct order using a yeast recombinational cloning system (28, 29). The first genetic element, corresponding to the 5′ *DHODH* target flank, was amplified from genomic DNA (~1.5 kbp). The 5′ *DHODH* target flank includes exon 1 and intron 1 of endogenous *TgDHODH*. The pET19b-WT, pET19b-N468A, pET19b-N468A, and pET19b-N365A/N468A expression plasmids were used to amplify the second genetic element, corresponding to DHODH cDNA (~1.2 kbp). The third genetic element, containing the hypoxanthine guanine phosphoribosyl transferase (HXGPRT) minigene cassette and 3′ gene flank of the endogenous *TgDHODH* gene (~2.8 kbp), was amplified from the previously described pΔDHOD plasmid (22) using a forward primer that inserted the hemagglutinin (HA) tag at the C terminus of *Tg*DHODH. Oligonucleotide primers used in PCR to construct gene replacement targeting plasmids are listed in Table S1 in the supplemental material. Gene-targeting plasmids were validated by restriction digest and by DNA sequencing to verify 100% homology in gene-targeting flanks.

Pyrimidine starvation assays. PFU assays were used to test pyrimidine starvation. Four 25-cm^2 HFF flasks were inoculated with ~500 PFU per strain. Parasites were allowed to invade for 2 h in uracil medium and were then rinsed with cold phosphate-buffered saline (PBS) to remove uracil and extracellular parasites. Two flasks were provided with fresh medium supplemented with uracil, and the remaining two flasks were incubated in medium lacking uracil to induce pyrimidine starvation. Cultures were incubated undisturbed for 7 days, and then monolayers were fixed, stained, and photographed.

Protein electrophoresis and immunoblots. SDS-polyacrylamide gel electrophoresis (SDS-PAGE) was carried out on 1-mm-thick gels, using 4 to 12% gradient NuPAGE precast bis-Tris gels and 1× MOPS (morpholinepropanesulfonic acid) SDS running buffer (Life Technologies). Electrophoresis was performed in a Hoefer SE260 small-format vertical electrophoresis system using a constant 160 V until the dye front crossed the stacking gel and then a constant 200 V until the dye front reached the gel bottom. Samples for immunoblots were prepared by resuspending a pellet of 1.5×10^8 tachyzoites in 40 μl lysis buffer containing 2× complete mini-protease inhibitor cocktail (Roche), 5 mM potassium phosphate (pH 7.0), 1 mM EDTA, 1 mM dithiothreitol (DTT), and 2% Triton X-100, and subjecting the solution to five freeze/thaw cycles. Lysates were centrifuged at 4°C and 16,000 × *g* for 20 min. Supernatants of lysed parasites were boiled for 10 min at 90°C in 4× NuPAGE lithium dodecyl sulfate (LDS) sample buffer (Life Technologies). Total protein concentration in supernatants of lysates were measured by the bicinchoninic acid (BCA) protein assay (Pierce) with bovine serum albumin (BSA) as the standard, using the microplate procedure performed according the manufacturer's instructions. Samples were electrotransferred from gels to nitrocellulose membranes (Millipore) using a Trans-Blot Turbo transfer system (Bio-Rad) for 50 min at 1.0 A with constant current. The blotted membrane was blocked with 5% nonfat dry milk in 1× TBS (10 mM Tris-HCl and 150 mM NaCl pH 7.4) containing 0.05% Tween 20 (TBS-T buffer) for 30 min. After washing the membrane 3 times with TBS-T, rat anti-HA monoclonal antibody (Roche) (100 ng/ml), diluted in TBS-T, was added and incubated overnight at 4°C. The bound antibodies were detected by horseradish peroxidase-conjugated (HRP) anti-rat IgG secondary antibody (Life Technologies) at a 1:10,000 dilution. Immunoreactive bands were visualized by enhanced chemiluminescence (ECL) using a Super-Signal West Pico chemiluminescent substrate kit (Pierce). The loading control for the Western blot was performed with primary mouse anti-ATP antibodies at a 1:5,000 dilution and a secondary anti-mouse IgG-HRP antibody. For quantification of proteins on Western blots, the density of bands was measured using Image J 1.48v (National Institutes of Health, USA; http://imagej.nih.gov/ij Java 1.6.0_65 [32-bit]). Protein expression levels were normalized to the loading control ATPase and reported as relative density expressed in arbitrary units.

Statistical analysis. All results were expressed as the mean ± standard error of the mean. A comparison between the two groups was performed using an unpaired Student *t* test. A P value of <0.05 was considered to indicate a statistically significant difference. All statistical analyses were performed using Graph Pad Prism version 7.0.

Immunofluorescence. Slides with intracellular parasites were prepared by growing human foreskin fibroblast (HFF) cells on eight-well glass Nunc Lab-Tek chamber slides (Thermo Scientific) for 24 h before infection (30). HFF cells on slides were infected with fresh *T. gondii* culture (4 μl) in invasion buffer (Eagle modified essential medium supplemented with 1% fetal bovine serum) and grown for 18 h. Parasites were fixed with 1× Histochoice (Amresco) for 20 min at room temperature (RT), permeabilized with 0.1% Triton X-100, blocked with 10% fetal bovine serum (FBS)–1% normal goat serum (NGS)–0.02% Triton-TX solution, and stained with primary antibodies (Rbα-HA, 1:400; Msα-ATPase, 1:5,000; Msα-ATrx1, 1:5,000) and 4′,6-diamino-2-phenylindole (DAPI) at 5 μg/ml. Msα-ATPase (monoclonal antibody [MAb] 5F4 [47]) and Msα-ATrx1 (MAb 11G8 [48]) were kindly provided by Peter J. Bradley (Department of Microbiology, Immunology and Molecular Genetics, University of California, Los Angeles, CA, USA). Secondary goat anti-mouse–Alexa-Fluor 594 and goat anti-rabbit–Alexa-Fluor 488 antibodies (Molecular Probes/Invitrogen) were used at 1:1,000. Slides were mounted

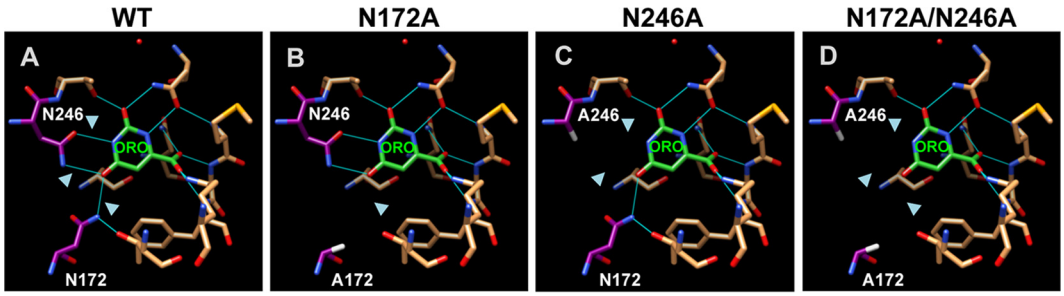

FIG 1 Views of the orotate binding site in wild-type and mutant *E. coli* DHODHs. The *E. coli* DHODH crystallographic structure (PDB ID: 1F76) was used to illustrate hydrogen bond interactions of orotate (green) with residues within 5 Å. (A) Hydrogen bonds predicted to form are shown in the wild-type enzyme. (B to D) Arrows indicate hydrogen bonds that are predicted to lose contact with orotate in enzymes with the single mutation N172A (B) or N246A (C) or in the N172A/N246A double mutant (D).

with Mowiol (Sigma) and examined on a Zeiss LSM 510 Meta laser-scanning confocal microscope with a 63× oil objective. All images were collected using the same settings for laser intensity, pinhole aperture, and photomultiplier gain and offset. MitoTracker stain was used to examine mitochondrial membrane potential. Parasite-infected cells were stained with 100 nM MitoTracker Red (CMXRos; Life Technologies) in normal growth medium (Dulbecco modified Eagle medium [DMEM] with 1% Cosmic calf serum) for 30 min at 37°C, and then cultures were examined for immunofluorescence as described above.

Expression and purification of N-terminally truncated wild-type and mutant DHODHs. Wild-type *T. gondii* DHODH and mutant enzymes (N365A, N468A, and N365A/N468A) were overexpressed in BL21-CodonPlus(DE3)RP cells (Stratagene) as previously described and purified as previously described with minor modifications (22). Briefly, cells were resuspended in buffer A (2 mM beta-mercaptoethanol, 2% Triton X-100, 10% glycerol, 0.5 mM riboflavin 5′-monophosphate [FMN], 300 mM NaCl, 50 mM Tris-HCl, pH 8.5) in the presence of 1 mM phenylmethylsulfonyl fluoride (PMSF), 1 mM benzamidine, and 1 mg/ml lysozyme and incubated for 3 h on ice. After sonication and centrifugation, recombinant proteins were purified using HisPur cobalt resin (Pierce) equilibrated with buffer B (buffer A with 5 mM imidazole). The column was washed with 15 mM imidazole, and proteins were eluted with 150 mM imidazole. Imidazole and excess FMN were removed using PD-10 desalting columns (Amersham) equilibrated with reaction buffer (150 mM KCl, 10% glycerol, 0.1% Triton, 50 mM Tris-HCl, pH 8.0). The protein concentration was measured using the microplate procedure of the bicinchoninic acid protein assay (Pierce) with bovine serum albumin as the standard, using a Thermo Scientific Multiskan GO microplate spectrophotometer.

Enzyme activity assays. Activities of wild-type and mutant recombinant *Tg*DHODH enzymes were measured by monitoring 2,6-dichlorophenol-indophenol (DCIP) reduction as previously described (22). Assays were performed in reaction buffer with 0.1 mM ubiquinone (Q_D) as an electron acceptor and 0.1 mM DCIP. Dihydroorotate (DHO) concentrations were varied from 0.5 to 50 mM to obtain substrate saturation curves. The following enzyme concentrations were used: 6.2 nM wild type, 1.86 μM N365A, 2.4 μM N468A, and 2.4 μM N365A/N468A. DCIP reduction was measured at 600 nm ($\varepsilon = 18{,}800\ M^{-1}cm^{-1}$) during 120 s at 2-s intervals for the wild-type enzyme and single mutants. N365A/N468A activity was measured for up to 10 min. All assays were performed in triplicate, using a Beckman Coulter DU 800 UV/visible spectrophotometer.

Bioinformatics. Molecular graphics images were produced using the UCSF Chimera package from the Resource for Biocomputing, Visualization, and Informatics at the University of California, San Francisco (http://www.cgl.ucsf.edu/chimera/). The *Escherichia coli* protein structure identified with the number PDB:1F76 was used for modeling.

RESULTS

Design of mutant *Tg*DHODH enzymes. DHODH oxidizes dihydroorotate to orotate with coordinate reduction of the enzyme-bound FMN in a stepwise reaction. Site-directed mutagenesis of several conserved asparagine (N) residues in *E. coli* DHODH adversely affected substrate or product binding as well as reduction rate constants (31). Mutation of N172 of *E. coli* DHODH caused a large decrease in the reduction rate constant with a slight decrease in dihydroorotate affinity, while mutation of N246 caused a large decrease in both kinetic parameters (31). Examination of the *E. coli* DHODH crystallographic structure shows that residues N172 and N246 are predicted to establish three hydrogen bonds with orotate (Fig. 1A) (20, 31). The N172A mutation abolishes one of these hydrogen bonds (Fig. 1B), the N246A mutation abolishes two of these hydrogen bonds (Fig. 1C), and the double mutation (DM) abolishes all three of these hydrogen bonds (Fig. 1D). We identified the conserved residues corresponding to *E. coli* DHODH N172 and N246 in *Tg*DHODH as N365 and N468 from previously reported ClustalW alignments of various DHODH proteins (22), and we hypothesized that mutation of either N365 or N468 in *Tg*DHODH would ablate enzyme activity.

Kinetic parameters of mutant *Tg*DHODH enzymes. Using a cDNA that expresses active N-terminally truncated wild-type *Tg*DHODH enzyme (22), we constructed three mutant *Tg*DHODH enzymes, N365A, N468A, and a N365A/N468A double mutant (DM). The bacterial expression vector pET19b was used to produce recombinant *Tg*DHODH proteins. Purified recombinant proteins of wild-type *Tg*DHODH or mutant enzymes were fractionated on SDS gels. As expected, the molecular mass observed for all the recombinants remained the same as that of the wild-type enzyme (~45 kDa) (Fig. 2A). Dihydroorotate oxidation was measured in the presence of the artificial electron acceptor Q_D using purified wild-type or mutant enzymes. The N365A and N468A mutants showed significant increases in K_m and significant decreases in k_{cat} (Fig. 2B and C). The kinetic efficiencies (k_{cat}/K_m) of the N365A and N468A mutant enzymes were reduced by 1,644-fold and by 296,000-fold, respectively, in comparison to that of the wild-type enzyme (Fig. 2C). Moreover, no detectable enzyme activity was observed for the DM enzyme. Attempts to obtain a detectable activity for the DM by increasing enzyme and substrate concentrations were unsuccessful. These results correlate with defects in kinetic parameters previously observed in the corresponding mutant *E. coli* DHODH enzymes (31), reinforcing the critical

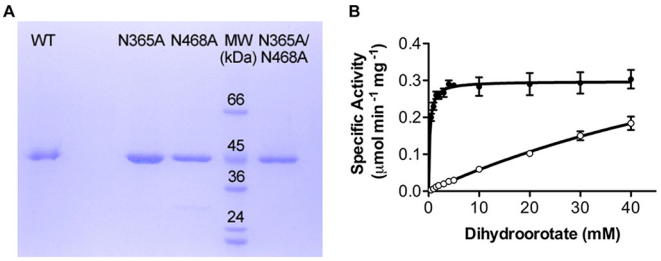

C

Enzyme	K_m (μM)	k_{cat} (s^{-1})	k_{cat}/K_m (s^{-1} μM^{-1})
Wild type	60 (± 0.003)	89 (± 1)	1.48 (±0.02)
N365A	256 (± 33)	0.240 (± 0.003)	0.0009 (±0.0001)
N468A	102500 (± 21100)	0.527 (± 0.084)	0.000005 (±0.000001)

FIG 2 Kinetic parameters of wild-type and mutant *T. gondii* DHODH enzymes. (A) SDS-PAGE showing the purified wild-type and mutant *Tg*DHODHs. (B) Dihydroorotate saturation curves of purified *Tg*DHODH mutants N365A (closed circles) and N468A (open circles). The concentration of Q_D was fixed at 0.1 mM, while the concentration of dihydroorotate was varied from 0 to 40 mM. Measurements for each point were in triplicate, and the background activity in the absence of enzyme was subtracted. (C) Michaelis constants, turnover numbers, and specificity constants for *Tg*DHODH active-site mutants and the wild-type enzyme.

importance of these asparagine residues in stabilizing the pyrimidine for efficient catalytic activity of family 2 DHODH enzymes.

Replacing the endogenous *TgDHODH* gene with mutant gene alleles. Several efforts to delete the *TgDHODH* gene were unsuccessful (22). However, the *TgDHODH* gene is not refractory to gene targeting, since this gene was successfully targeted at its chromosomal locus to generate a C-terminally HA-tagged *Tg*DHODH to demonstrate mitochondrial localization of *Tg*DHODH (22). Together, these results suggested that the *Tg*DHODH protein could have a second essential function in the mitochondria that is independent of its predicted role in *T. gondii* pyrimidine biosynthesis. We hypothesized that expression of a *Tg*DHODH protein deficient in enzyme activity and simultaneous deletion of the endogenous *TgDHODH* gene may enable the rescue of the unknown second mitochondrial function of *Tg*DHODH, creating a mutant phenotype of uracil auxotrophy that can be rescued *in vitro* by supplementation of the growth medium with uracil.

The wild-type *TgDHODH* or the engineered single mutant or double mutant gene alleles, all C-terminally tagged with HA, were targeted to the endogenous *TgDHODH* gene locus to simultaneously delete and replace the endogenous *TgDHODH* gene. The strategy for gene replacement used previously engineered plasmids expressing the recombinant *Tg*DHODH proteins (Fig. 2); however, integration of the targeting plasmid at the *TgDHODH* gene locus was designed to rescue the complete coding region of *Tg*DHODH or the mutant enzymes (Fig. 3A). Progeny were selected in mycophenolic acid plus xanthine plus uracil. Several progeny with the correct genotype of the targeted gene replacement were validated using a PCR strategy to demonstrate correct 5′ and 3′ integration of the 5′ and 3′ target DNA flanks carried on the targeting plasmid (PCR4 and PCR5), the presence of the plasmid-targeted *TgDHODH* gene in the endogenous *TgDHODH* chromosomal locus (PCR2B* and PCR4), and the absence of the

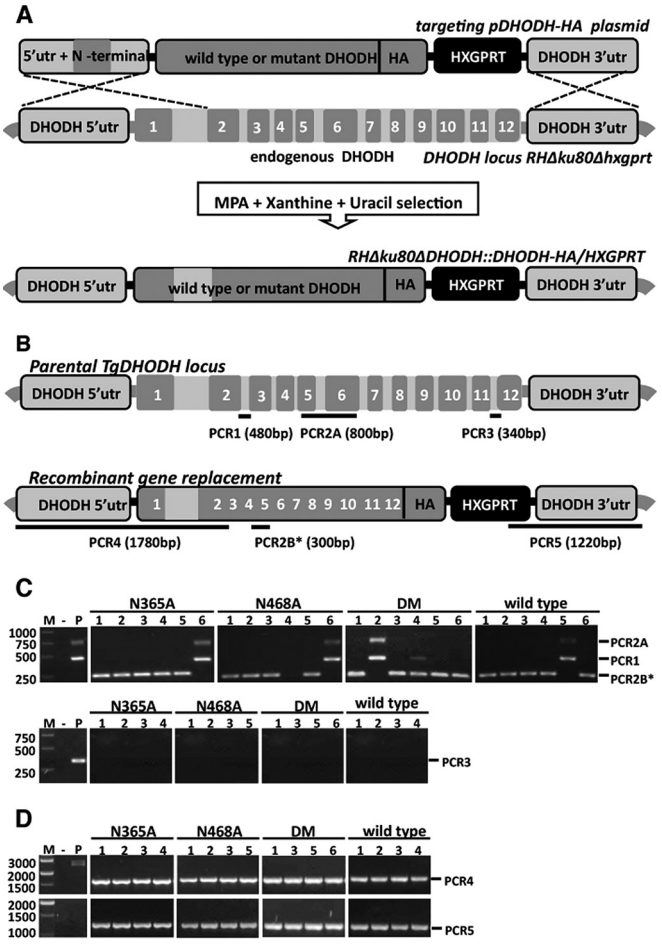

FIG 3 Gene replacements at the endogenous *TgDHODH* gene locus. (A) Top, gene-targeting plasmids were engineered to contain the 5′ *DHODH* target flank, the wild-type or mutant *TgDHODH* gene containing a C-terminal HA tag, the *HXGPRT* selectable marker, and the 3′ *DHODH* target flank. Bottom, the endogenous *TgDHODH* gene (light and dark gray box) was targeted for gene replacement using linearized targeting plasmid. The 12 coding exons in the endogenous gene are shown by white numbers (1 to 12). The N terminus (exon 1 and intron 1), missing in the targeting plasmid constructs, was rescued by correct integration into the endogenous *TgDHODH* gene locus following selection in mycophenolic acid (MPA) plus xanthine plus uracil. (B) Schematic representation of the PCR genotype validation scheme. Approximate locations of PCR products used to validate genotypes are shown. (C) Representative clones showing correct gene replacements for N365A, N468A, DM, and wild-type *Tg*DHODHs. Strains with correct integration of the mutated DHODH construct were positive only for PCR2B (300 bp). The parental strain RH Δ*ku80* Δ*hxgprt* (endogenous *TgDHODH* gene locus) was positive for PCR1 (480 bp) and PCR2 (800 bp). The lack of PCR amplification observed for PCR3 confirms excision of the endogenous gene. (D) Representative clones showing correct gene replacements for N365A, N468A, DM, and wild-type *Tg*DHODHs. Strains with correct 5′ integration (PCR4, 1,780 bp) and 3′ integration (PCR5, 1,220 bp) are shown. Lanes: M, standard size markers; −, negative control; P, parental strain; 1 to 6, clones tested per strain.

endogenous *TgDHODH* gene (PCR1, PCR2A, and PCR3) (Fig. 3B and C). In addition, Western blots using anti-HA antibody demonstrated expression of the HA-tagged *Tg*DHODH products from the wild type, the single mutants, or the DM (Fig. 4A). Relative to the ATPase control, expression of the DM was reduced in comparison to those of N468A and the wild-type *Tg*DHODH (Fig. 4B).

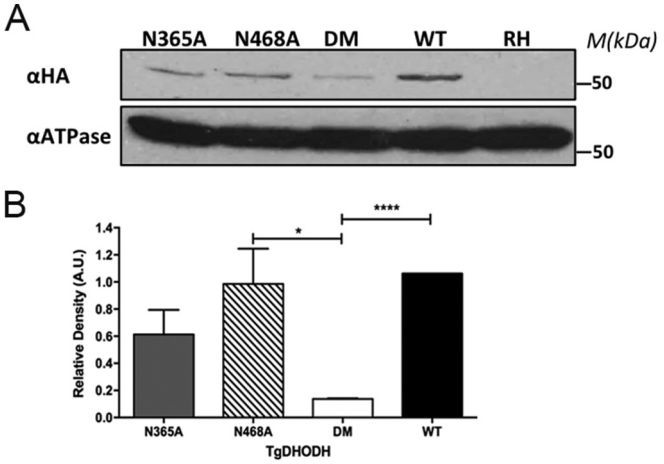

FIG 4 Tachyzoites of *T. gondii* express mutated DHODHs. (A) Western blotting was performed using lysed tachyzoites from endogenously HA-tagged wild-type (WT), N365A, N468A, and DM strains. The parental strain was used as a negative control. Anti-HA antibodies (top) recognize a band of ~50 kDa in the three *Tg*DHODH mutants and the wild-type *Tg*DHODH but not in the nontagged parental strain. The mitochondrial marker ATP synthase (anti-ATPase antibodies) (bottom) was used as a standard for sample loading. (B) Relative expression level of *Tg*DHODH compared to ATPase. Three replicate Western blots were analyzed using ATPase as the standard for expression level. Protein expression level is reported as relative density and is expressed in arbitrary units. Values are means ± standard errors of the means (SEM). ****, $P < 0.0001$ for VSSM versus DM; *, $P < 0.05$ for N468A versus DM.

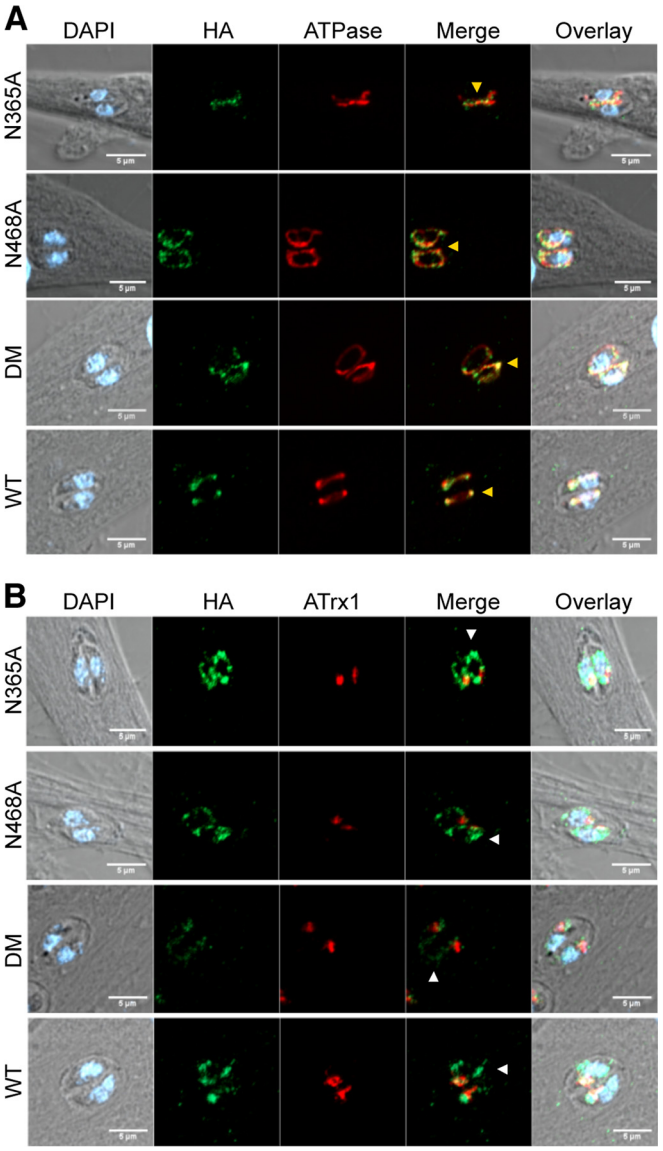

FIG 5 Subcellular localization of mutant *Tg*DHODH enzymes. (A) Intracellular tachyzoites expressing mutant HA-tagged *Tg*DHODH were used in double-staining immunofluorescence with anti-HA (green) and the mitochondrial marker ATP synthase (anti-ATPase) (red). Nuclei were stained with DAPI (blue). Yellow arrows show colocalization of mutant or wild-type (WT) *Tg*DHODH with mitochondrial ATP synthase (merge panel). (B) Staining immunofluorescence using antibodies against HA (anti-HA) (green) and the apicoplast marker ATrx1 (anti-ATrx1) (red). Nuclei were stained with DAPI (blue). White arrows show no colocalization of HA with ATrx1.

Wild-type and mutant *Tg*DHODH enzymes localize to the parasite mitochondria. *Tg*DHODH localizes to mitochondria (22). The *T. gondii* strains carrying wild-type or mutant *DHODH* gene replacements at the endogenous *TgDHODH* locus were evaluated to examine the cellular localization of *Tg*DHODH. As expected, HA-tagged *Tg*DHODH colocalized with the mitochondrial marker ATPase (Fig. 5A) and was not localized with the apicoplast marker ATrx1 (Fig. 5B), showing correct localization of the mutant enzymes to the mitochondrion.

Enzyme activity-deficient *Tg*DHODH mutants are uracil auxotrophs. To determine if ablation of DHODH activity induced pyrimidine auxotrophy, the mutant or wild-type strains were subjected to plaque assays in the presence or absence of uracil supplementation. The strain with the catalytically active wild-type *TgDHODH* gene allele replicated to form plaques with or without uracil supplementation. In contrast, the single mutant strains as well as the DM strain were uracil auxotrophs and did not replicate to develop plaques in the absence of uracil supplementation (Fig. 6).

Mutant *Tg*DHODH strains contain active mitochondria. MitoTracker Red CMXRos is an indicator that stains mitochondria in living cells, and staining depends on the presence of a functional membrane potential (32). Wild-type and mutant strains were cultured in the presence of uracil to obtain intracellular parasite vacuoles, and vacuoles were stained with MitoTracker to examine whether fluorescence was associated with parasite mitochondria. *T. gondii* actively recruits host cell mitochondria to the surface membrane of the parasitophorous vacuole (PVM) (33); consequently, MitoTracker will stain host mitochondria associated with the PVM as well as parasite mitochondria associated with each tachyzoite inside the vacuole. MitoTracker stained both parasite and host mitochondria, and the staining patterns were identical in the wild-type and mutant DHODH strains (Fig. 7), suggesting that inactivation of the *Tg*DHODH enzyme activity did not significantly affect the membrane potential of parasite mitochondria or PVM-associated host mitochondria (Fig. 7).

DISCUSSION

Pyrimidine biosynthesis is an essential pathway in *T. gondii*. Previous genetic studies in *T. gondii* have shown that deletion of the gene(s) encoding the first, fifth, or sixth steps of the pyrimidine biosynthetic pathway in *T. gondii* induced uracil auxotrophy and virulence attenuation and abolished chronic infection of the host (16–19), suggesting that inhibitors of *Tg*DHODH could be active

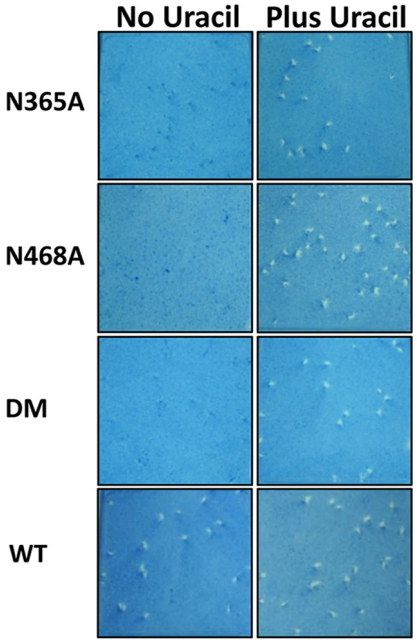

FIG 6 Catalytically deficient mutant *Tg*DHODH strains are uracil auxotrophs. The wild-type (WT) strain and three catalytically deficient *Tg*DHODH mutant strains (N365A, N468A, and DM) were grown in the absence (left) or in the presence (right) of uracil supplementation, and plaques were measured 7 days later. Uracil auxotrophy was observed in the mutants.

against both acute and chronic stages of infection. However, attempts to directly delete the *TgDHODH* gene were unsuccessful. Here, we show that replacement of the endogenous *TgDHODH* gene with a catalytically deficient mutant *TgDHODH* gene allele was sufficient to establish uracil auxotrophy. These findings show that *Tg*DHODH is essential for the synthesis of pyrimidines and participates in another essential mitochondrial function that is not directly dependent on *Tg*DHODH enzyme activity in the pyrimidine biosynthetic pathway.

The enzyme activity of DHODH has been a highly investigated target for the development of inhibitors used to treat autoimmune diseases and for their use in treatments for cancer and virus and parasitic infections (34). In particular, significant progress has been made in identifying clinically relevant inhibitors of the *Plasmodium* DHODH that show promise for further clinical development in malaria treatment (10, 11). We have previously reported an initial screen of potential inhibitors of *Tg*DHODH, and several micromolar inhibitors were identified (22). However, the search for inhibitors of the *T. gondii* enzyme has been hindered by the absence of a crystal structure for this enzyme. Our results using mutagenesis and protein expression assays confirm the predicted active-site residues of the *Tg*DHODH. The N365A mutation increased the K_m for dihydroorotate and severely reduced the k_{cat}, while the N468A mutation severely affected both kinetic parameters. Enzyme activity was not detected in the double mutant. Overall, these impaired kinetic properties of *Tg*DHODH activity are consistent with previous mutagenesis studies performed on corresponding mutations developed in the *E. coli* DHODH (31) and reinforce the importance of these key asparagine residues in catalysis. *Tg*DHODH differs from other family 2 DHODHs in containing an extended N-terminal targeting sequence of 157 amino acids that appears to be cleaved during mitochondrial import (22). In contrast, the human *Hs*DHODH contains only a short N-terminal sequence (13 amino acid residues) that is not removed (21). *Tg*DHODH also displays an internal insertion of approximately 20 to 30 amino acid residues, a novel characteristic

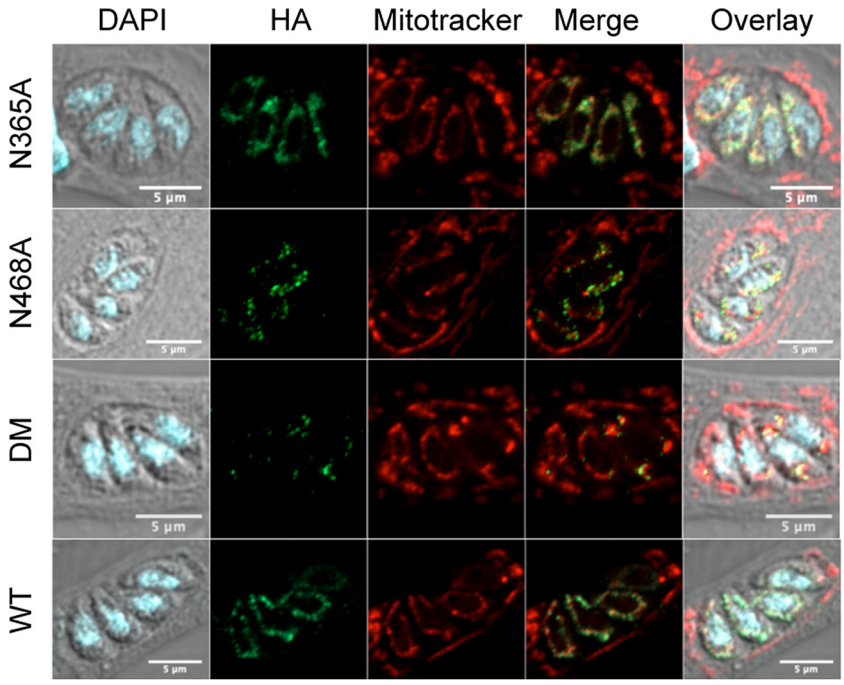

FIG 7 Catalytically deficient mutant *Tg*DHODH strains contain active mitochondria. MitoTracker retention in the mitochondria (red) was tested on nonfixed intracellular wild-type (WT) or mutant *Tg*DHODH parasites. *Tg*DHODH was localized with anti-HA antibody (green). Nuclei were stained with DAPI (blue).

that it shares with *Plasmodium* DHODH enzymes (22). However, this insertion in the *Plasmodium* DHODH was not required for catalytic activity (35). It remains to be examined whether this novel insertion is required for the pyrimidine-independent role of *Tg*DHODH.

Our results confirm the expected essential enzyme activity of *Tg*DHODH in pyrimidine biosynthesis and point to the presence of a second essential function for *Tg*DHODH that is independent of the enzyme activity. Pyrimidine biosynthesis is coupled to the respiratory chain by the participation of ubiquinone in the reoxidation of DHODH, and the electrons generated from dihydroorotate oxidation are transferred into the respiratory chain (24). *T. gondii* and blood stages of malaria parasites both require mitochondrial metabolism, because these parasites are highly susceptible to inhibitors of cytochrome bc_1 (complex III), such as atovaquone (36–38), that inhibit electron transport through the essential respiratory chain (39–41). Recent studies on mammalian DHODH have shown that DHODH is physically associated with the respiratory chain complexes III and II (42). Moreover, depletion of DHODH induced cell cycle arrest and mitochondrial dysfunction (42–44). Here, we show that wild-type and mutant *Tg*DHODH enzymes localized to the parasite mitochondria and that *T. gondii* expressing catalytically deficient DHODH retained an intact mitochondrial membrane potential even with reduced expression levels of catalytically deficient *Tg*DHODH enzymes. These observations suggest that the pyrimidine biosynthetic function of *Tg*DHODH is not strictly required for maintaining the essential respiratory chain in *T. gondii*, though our results should be interpreted cautiously because MitoTracker staining may not reveal a reduced membrane potential in contrast to a collapsed membrane potential. Collectively, our findings point to a novel and essential role for *Tg*DHODH in mitochondrial function and physiology that is independent of pyrimidine biosynthesis. These findings are important for future drug development because they suggest that inhibitors of the *Tg*DHODH molecule could block an essential enzymatic step in pyrimidine biosynthesis as well as block an essential function of *Tg*DHODH in mitochondrial physiology. Identifying selective inhibitors of *Tg*DHODH as well as the molecular basis of the pyrimidine-independent role for *Tg*DHODH merits further investigation.

ACKNOWLEDGMENTS

This work was supported by NIH grant AI041930 (D.J.B.). ToxoDB, PlasmoDB, and EuPathDB are part of the NIH/NIAID-funded Bioinformatics Resource Center.

We gratefully acknowledge the valuable work of the developers of the *Toxoplasma gondii* Genome Resource at www.ToxoDB.org. We thank Peter J. Bradley for providing mitochondrial and apicoplast-specific antibodies.

FUNDING INFORMATION

This work, including the efforts of David J. Bzik, was funded by HHS | National Institutes of Health (NIH) (AI041930).

REFERENCES

1. **Dubey JP.** 2007. The history and life cycle of Toxoplasma gondii, p 1–18. *In* Weiss LM, Kim K (ed), Toxoplasma gondii: the model apicomplexan parasite: perspectives and methods. Elsevier, London, United Kingdom.
2. **Montoya JG, Remington JS.** 2008. Management of Toxoplasma gondii infection during pregnancy. Clin Infect Dis **47:**554–566. http://dx.doi.org/10.1086/590149.
3. **Jones JL, Holland GN.** 2010. Annual burden of ocular toxoplasmosis in the US. Am J Trop Med Hyg **82:**464–465. http://dx.doi.org/10.4269/ajtmh.2010.09-0664.
4. **Luft BJ, Remington JS.** 1992. Toxoplasmic encephalitis in AIDS. Clin Infect Dis **15:**211–222. http://dx.doi.org/10.1093/clinids/15.2.211.
5. **Schmidt DR, Hogh B, Andersen O, Hansen SH, Dalhoff K, Petersen E.** 2006. Treatment of infants with congenital toxoplasmosis: tolerability and plasma concentrations of sulfadiazine and pyrimethamine. Eur J Pediatr **165:**19–25. http://dx.doi.org/10.1007/s00431-005-1665-4.
6. **Hyde JE.** 2007. Targeting purine and pyrimidine metabolism in human apicomplexan parasites. Curr Drug Targets **8:**31–47. http://dx.doi.org/10.2174/138945007779315524.
7. **Fox BA, Bzik DJ.** 2003. Organisation and sequence determination of glutamine-dependent carbamoyl phosphate synthetase II in Toxoplasma gondii. Int J Parasitol **33:**89–96. http://dx.doi.org/10.1016/S0020-7519(02)00214-X.
8. **Rathod PK, Reyes P.** 1983. Orotidylate-metabolizing enzymes of the human malarial parasite, Plasmodium falciparum, differ from host cell enzymes. J Biol Chem **258:**2852–2855.
9. **Reyes P, Rathod PK, Sanchez DJ, Mrema JE, Rieckmann KH, Heidrich HG.** 1982. Enzymes of purine and pyrimidine metabolism from the human malaria parasite, Plasmodium falciparum. Mol Biochem Parasitol **5:**275–290. http://dx.doi.org/10.1016/0166-6851(82)90035-4.
10. **Phillips MA, Lotharius J, Marsh K, White J, Dayan A, White KL, Njoroge JW, El Mazouni F, Lao Y, Kokkonda S, Tomchick DR, Deng X, Laird T, Bhatia SN, March S, Ng CL, Fidock DA, Wittlin S, Lafuente-Monasterio M, Benito FJ, Alonso LM, Martinez MS, Jimenez-Diaz MB, Bazaga SF, Angulo-Barturen I, Haselden JN, Louttit J, Cui Y, Sridhar A, Zeeman AM, Kocken C, Sauerwein R, Dechering K, Avery VM, Duffy S, Delves M, Sinden R, Ruecker A, Wickham KS, Rochford R, Gahagen J, Iyer L, Riccio E, Mirsalis J, Bathhurst I, Rueckle T, Ding X, Campo B, Leroy D, Rogers MJ, Rathod PK, Burrows JN, Charman SA.** 2015. A long-duration dihydroorotate dehydrogenase inhibitor (DSM265) for prevention and treatment of malaria. Sci Transl Med **7:**296ra111. http://dx.doi.org/10.1126/scitranslmed.aaa6645.
11. **Kokkonda S, Deng X, White KL, Coteron JM, Marco M, de Las Heras L, White J, El Mazouni F, Tomchick DR, Manjalanagara K, Rudra KR, Chen G, Morizzi J, Ryan E, Kaminsky W, Leroy D, Martinez-Martinez MS, Jimenez-Diaz MB, Bazaga SF, Angulo-Barturen I, Waterson D, Burrows JN, Matthews D, Charman SA, Phillips MA, Rathod PK.** 2016. Tetrahydro-2-naphthyl and 2-indanyl triazolopyrimidines targeting Plasmodium falciparum dihydroorotate dehydrogenase display potent and selective antimalarial activity. J Med Chem http://dx.doi.org/10.1021/acs.jmedchem.6b00275.
12. **Schwartzman JD, Pfefferkorn ER.** 1981. Pyrimidine synthesis by intracellular Toxoplasma gondii. J Parasitol **67:**150–158. http://dx.doi.org/10.2307/3280627.
13. **Iltzsch MH.** 1993. Pyrimidine salvage pathways in Toxoplasma gondii. J Eukaryot Microbiol **40:**24–28. http://dx.doi.org/10.1111/j.1550-7408.1993.tb04877.x.
14. **Pfefferkorn ER.** 1978. Toxoplasma gondii: the enzymic defect of a mutant resistant to 5-fluorodeoxyuridine. Exp Parasitol **44:**26–35. http://dx.doi.org/10.1016/0014-4894(78)90077-2.
15. **Donald RG, Roos DS.** 1995. Insertional mutagenesis and marker rescue in a protozoan parasite: cloning of the uracil phosphoribosyltransferase locus from Toxoplasma gondii. Proc Natl Acad Sci U S A **92:**5749–5753. http://dx.doi.org/10.1073/pnas.92.12.5749.
16. **Fox BA, Bzik DJ.** 2015. Nonreplicating, cyst-defective type II Toxoplasma gondii vaccine strains stimulate protective immunity against acute and chronic infection. Infect Immun **83:**2148–2155. http://dx.doi.org/10.1128/IAI.02756-14.
17. **Fox BA, Bzik DJ.** 2002. De novo pyrimidine biosynthesis is required for virulence of Toxoplasma gondii. Nature **415:**926–929. http://dx.doi.org/10.1038/415926a.
18. **Fox BA, Bzik DJ.** 2010. Avirulent uracil auxotrophs based on disruption of orotidine-5′-monophosphate decarboxylase elicit protective immunity to Toxoplasma gondii. Infect Immun **78:**3744–3752. http://dx.doi.org/10.1128/IAI.00287-10.
19. **Fox BA, Falla A, Rommereim LM, Tomita T, Gigley JP, Mercier C, Cesbron-Delauw MF, Weiss LM, Bzik DJ.** 2011. Type II Toxoplasma gondii KU80 knockout strains enable functional analysis of genes required for cyst development and latent infection. Eukaryot Cell **10:**1193–1206. http://dx.doi.org/10.1128/EC.00297-10.
20. **Norager S, Jensen KF, Bjornberg O, Larsen S.** 2002. E. coli dihydrooro-

tate dehydrogenase reveals structural and functional distinctions between different classes of dihydroorotate dehydrogenases. Structure **10:**1211–1223. http://dx.doi.org/10.1016/S0969-2126(02)00831-6.

21. **Rawls J, Knecht W, Diekert K, Lill R, Loffler M.** 2000. Requirements for the mitochondrial import and localization of dihydroorotate dehydrogenase. Eur J Biochem **267:**2079–2087. http://dx.doi.org/10.1046/j.1432-1327.2000.01213.x.
22. **Hortua Triana MA, Huynh MH, Garavito MF, Fox BA, Bzik DJ, Carruthers VB, Loffler M, Zimmermann BH.** 2012. Biochemical and molecular characterization of the pyrimidine biosynthetic enzyme dihydroorotate dehydrogenase from Toxoplasma gondii. Mol Biochem Parasitol **184:**71–81. http://dx.doi.org/10.1016/j.molbiopara.2012.04.009.
23. **Krungkrai J.** 1995. Purification, characterization and localization of mitochondrial dihydroorotate dehydrogenase in Plasmodium falciparum, human malaria parasite. Biochim Biophys Acta **1243:**351–360. http://dx.doi.org/10.1016/0304-4165(94)00158-T.
24. **Rowland P, Nielsen FS, Jensen KF, Larsen S.** 1997. The crystal structure of the flavin containing enzyme dihydroorotate dehydrogenase A from Lactococcus lactis. Structure **5:**239–252. http://dx.doi.org/10.1016/S0969-2126(97)00182-2.
25. **Fox BA, Gigley JP, Bzik DJ.** 2004. Toxoplasma gondii lacks the enzymes required for de novo arginine biosynthesis and arginine starvation triggers cyst formation. Int J Parasitol **34:**323–331. http://dx.doi.org/10.1016/j.ijpara.2003.12.001.
26. **Gigley JP, Fox BA, Bzik DJ.** 2009. Cell-mediated immunity to Toxoplasma gondii develops primarily by local Th1 host immune responses in the absence of parasite replication. J Immunol **182:**1069–1078. http://dx.doi.org/10.4049/jimmunol.182.2.1069.
27. **Fox BA, Ristuccia JG, Gigley JP, Bzik DJ.** 2009. Efficient gene replacements in Toxoplasma gondii strains deficient for nonhomologous end joining. Eukaryot Cell **8:**520–529. http://dx.doi.org/10.1128/EC.00357-08.
28. **Oldenburg KR, Vo KT, Michaelis S, Paddon C.** 1997. Recombination-mediated PCR-directed plasmid construction in vivo in yeast. Nucleic Acids Res **25:**451–452. http://dx.doi.org/10.1093/nar/25.2.451.
29. **Rommereim LM, Hortua Triana MA, Falla A, Sanders KL, Guevara RB, Bzik DJ, Fox BA.** 2013. Genetic manipulation in Deltaku80 strains for functional genomic analysis of Toxoplasma gondii. J Vis Exp http://dx.doi.org/10.3791/50598.
30. **Huynh MH, Rabenau KE, Harper JM, Beatty WL, Sibley LD, Carruthers VB.** 2003. Rapid invasion of host cells by Toxoplasma requires secretion of the MIC2-M2AP adhesive protein complex. EMBO J **22:**2082–2090. http://dx.doi.org/10.1093/emboj/cdg217.
31. **Fagan RL, Palfey BA.** 2009. Roles in binding and chemistry for conserved active site residues in the class 2 dihydroorotate dehydrogenase from Escherichia coli. Biochemistry **48:**7169–7178. http://dx.doi.org/10.1021/bi900370s.
32. **Pendergrass W, Wolf N, Poot M.** 2004. Efficacy of MitoTracker Green and CMXrosamine to measure changes in mitochondrial membrane potentials in living cells and tissues. Cytometry A **61:**162–169.
33. **Pernas L, Adomako-Ankomah Y, Shastri AJ, Ewald SE, Treeck M, Boyle JP, Boothroyd JC.** 2014. Toxoplasma effector MAF1 mediates recruitment of host mitochondria and impacts the host response. PLoS Biol **12:**e1001845. http://dx.doi.org/10.1371/journal.pbio.1001845.
34. **Munier-Lehmann H, Vidalain PO, Tangy F, Janin YL.** 2013. On dihydroorotate dehydrogenases and their inhibitors and uses. J Med Chem **56:**3148–3167. http://dx.doi.org/10.1021/jm301848w.
35. **Deng X, Gujjar R, El Mazouni F, Kaminsky W, Malmquist NA, Goldsmith EJ, Rathod PK, Phillips MA.** 2009. Structural plasticity of malaria dihydroorotate dehydrogenase allows selective binding of diverse chemical scaffolds. J Biol Chem **284:**26999–27009. http://dx.doi.org/10.1074/jbc.M109.028589.
36. **Araujo FG, Huskinson-Mark J, Gutteridge WE, Remington JS.** 1992. In vitro and in vivo activities of the hydroxynaphthoquinone 566C80 against the cyst form of Toxoplasma gondii. Antimicrob Agents Chemother **36:**326–330. http://dx.doi.org/10.1128/AAC.36.2.326.
37. **Fry M, Pudney M.** 1992. Site of action of the antimalarial hydroxynaphthoquinone, 2-[trans-4-(4′-chlorophenyl) cyclohexyl]-3-hydroxy-1,4-naphthoquinone (566C80). Biochem Pharmacol **43:**1545–1553. http://dx.doi.org/10.1016/0006-2952(92)90213-3.
38. **Mather MW, Darrouzet E, Valkova-Valchanova M, Cooley JW, McIntosh MT, Daldal F, Vaidya AB.** 2005. Uncovering the molecular mode of action of the antimalarial drug atovaquone using a bacterial system. J Biol Chem **280:**27458–27465. http://dx.doi.org/10.1074/jbc.M502319200.
39. **Miley GP, Pou S, Winter R, Nilsen A, Li Y, Kelly JX, Stickles AM, Mather MW, Forquer IP, Pershing AM, White K, Shackleford D, Saunders J, Chen G, Ting LM, Kim K, Zakharov LN, Donini C, Burrows JN, Vaidya AB, Charman SA, Riscoe MK.** 2015. ELQ-300 prodrugs for enhanced delivery and single-dose cure of malaria. Antimicrob Agents Chemother **59:**5555–5560. http://dx.doi.org/10.1128/AAC.01183-15.
40. **Painter HJ, Morrisey JM, Mather MW, Vaidya AB.** 2007. Specific role of mitochondrial electron transport in blood-stage Plasmodium falciparum. Nature **446:**88–91. http://dx.doi.org/10.1038/nature05572.
41. **Vaidya AB, Painter HJ, Morrisey JM, Mather MW.** 2008. The validity of mitochondrial dehydrogenases as antimalarial drug targets. Trends Parasitol **24:**8–9. http://dx.doi.org/10.1016/j.pt.2007.10.005.
42. **Fang J, Uchiumi T, Yagi M, Matsumoto S, Amamoto R, Takazaki S, Yamaza H, Nonaka K, Kang D.** 2013. Dihydro-orotate dehydrogenase is physically associated with the respiratory complex and its loss leads to mitochondrial dysfunction. Biosci Rep **33:**e00021. http://dx.doi.org/10.1042/BSR20120097.
43. **Fang J, Uchiumi T, Yagi M, Matsumoto S, Amamoto R, Saito T, Takazaki S, Kanki T, Yamaza H, Nonaka K, Kang D.** 2012. Protein instability and functional defects caused by mutations of dihydro-orotate dehydrogenase in Miller syndrome patients. Biosci Rep **32:**631–639. http://dx.doi.org/10.1042/BSR20120046.
44. **Fang J, Yamaza H, Uchiumi T, Hoshino Y, Masuda K, Hirofuji Y, Wagener FA, Kang D, Nonaka K.** 2016. Dihydroorotate dehydrogenase depletion hampers mitochondrial function and osteogenic differentiation in osteoblasts. Eur J Oral Sci **124:**241–245. http://dx.doi.org/10.1111/eos.12270.